

Gene Expression Profiles Define a Key Checkpoint for Type 1 Diabetes in NOD Mice

Sarah E. Eckenrode, Qingguo Ruan, Ping Yang, Weipeng Zheng, Richard A. McIndoe, and Jin-Xiong She

cDNA microarrays with >11,000 cDNA clones from an NOD spleen cDNA library were used to identify temporal gene expression changes in NOD mice (1–10 weeks), which spontaneously develop type 1 diabetes, and changes between NOD and NOD congenic mice (NOD.Idd3/Idd10 and NOD.B10Sn-H2^b), which have near zero incidence of insulinitis and diabetes. The expression profiles identified two distinct groups of mice corresponding to an immature (1–4 weeks) and mature (6–10 weeks) state. The rapid switch of gene expression occurring around 5 weeks of age defines a key immunological checkpoint. Sixty-two known genes are upregulated, and 18 are downregulated at this checkpoint in the NOD. The expression profiles are consistent with increased antibody production, antigen presentation, and cell proliferation associated with an active autoimmune response. Seven of these genes map to confirmed diabetes susceptibility regions. Of these seven, three are excellent candidate genes not previously implicated in type 1 diabetes. Ten genes are differentially expressed between the NOD and congenic NOD at the immature stage (*Hspa8*, *Hif1a*, and several involved in cellular functions), while the other 70 genes exhibit expression differences during the mature (6–10 week) stage, suggesting that the expression differences of a small number of genes before onset of insulinitis determine the disease progression. *Diabetes* 53:366–375, 2004

Type 1 diabetes is a disease manifested when the insulin-producing pancreatic β -cells are destroyed by the immune system. Studies using the NOD mouse model, which spontaneously develops type 1 diabetes, have shown that both B- and T-cells are necessary for the development of the disease (1–5). Other immune cells, such as macrophages and dendritic cells, have also been implicated in the disease process (6). Despite extensive studies on this animal model, the underlying molecular mechanisms that lead to the development and progression of type 1 diabetes remain elusive.

Previous studies primarily focused on one or a few molecules believed to be involved in the disease pathogen-

esis. The information obtained from these experiments is ideal for uncovering the role of specific genes. However, the single gene approach is not the ideal way to discover new genes or the molecular networks involved in the disease process. The conventional approaches of investigation have limited the rate of progress because of the complex nature of this disease. The recent development of microarray technology has provided a high-throughput approach to simultaneously analyze the expression of tens of thousands of genes. This genomic revolution has fundamentally changed how investigators can approach biomedical questions.

Several studies have used the microarray approach to study gene expression in islet cells (7–9) and immune cells (10,11). Because of the preliminary nature of the published studies on the immune system, few definitive conclusions were reached. In this study, microarray technology was used to extensively profile splenic gene expression of NOD mice at different ages. Analysis of the longitudinal expression profiles from the NOD splenic cells helped establish disease stages based on patterns of gene expression. These expression patterns were compared with those generated from age-matched NOD congenic mice, NOD.Idd3/Idd10 and NOD.B10Sn-H2^b, which have a decreased incidence of insulinitis and diabetes. We present here the major findings from this extensive microarray dataset of 117 mouse spleens.

RESEARCH DESIGN AND METHODS

Mice. NOD/LtJ, NOD.B10Sn-H2^b, and C57BL/6J (B6) mice were purchased from The Jackson Laboratory and then housed and bred under specific-pathogen-free conditions following the Committee on Animal Use for Research and Education (IACUC) guidelines at the University of Florida. The NOD.Idd3/Idd10 breeders were a gift from Dr. Edward Leiter. The NOD.B10Sn-H2^b and NOD.Idd3/Idd10 mice have been back-crossed for 15 and 11 generations, respectively. Only female mice were used in this study.

Library construction. Total RNA (RNeasy Midi Kit, Qiagen) and then mRNA [Poly(A)Pure kit, Ambion] were isolated from multiple spleens of NOD and B6 female mice at 10 weeks of age. Three micrograms from each pool was used to create the library with the PCR-Select cDNA Subtraction Kit (BD Biosciences Clontech) (12) and then cloned into pCR2.1 vectors (TA cloning, Invitrogen). Each clone was amplified by PCR. Briefly, each reaction contained 22 μ l 100 mmol/l dNTP, 11 μ l 10 \times PCR buffer, 2.2 μ l 20 pmol/ μ l TA-F primer (5'CCGCCAGTGTGATGGATATCTG), 2.2 μ l 20 pmol/ μ l TA-R primer (5'TCCACTAGTAACGGCCGCCAG), 0.8 μ l *Taq* polymerase, and 61.7 μ l deionized water. This mixture was subjected to 40 cycles of 94°C for 30 s, 64°C for 30 s, and 72°C for 1 min. The PCR product was isopropanol precipitated then resuspended in 20 μ l of 150 mmol/l sodium phosphate buffer (combine 1.1 ml 150 mmol/l NaH₂PO₄, 48.9 ml 150 mmol/l Na₂HPO₄, and 50 μ l 10% SDS, then pH to 8.5).

Printing of mouse array 1 microarrays. Clear microscope slides were cleaned in a sodium hydroxide/ethanol solution (70g NaOH dissolved in 280 ml deionized water, to which 420 ml of 95% ethanol was slowly added) for 2 h. After a thorough rinsing, the slides were placed for 1 h in poly-L-lysine solution (560 ml deionized water with 70 ml poly-L-lysine and 70 ml PBS). The slides

From the Center for Biotechnology and Genomic Medicine, Medical College of Georgia, Augusta, Georgia.

S.E.E. and Q.R. contributed equally to this work.

Address correspondence and reprint requests to Dr. Jin-Xiong She, Center for Biotechnology and Genomic Medicine, Medical College of Georgia, 1120 15th Street, PV6B108, Augusta, GA 30912-2400. E-mail: jshe@mail.mcg.edu.

Received for publication 11 July 2003 and accepted in revised form 5 November 2003.

B6, C57BL/6J mouse; DEPC, diethyl pyrocarbonate; MAR1, mouse array 1. © 2004 by the American Diabetes Association.

TABLE 1
Numbers of mice used in experiments

	Age (weeks)									
	1	2	3	4	5	6	7	8	10	
NOD	3	7	8	16	8	4	2	4	9	
NOD.Idd3/Idd10	—	—	7	4	—	4	—	1	8	
NOD.B10Sn-H2 ^b	—	—	18	4	—	5	—	—	5	

were briefly rinsed, centrifuged dry, and aged at least 3 days before printing. The MicroGrid TAS II (BioRobotics) was used to print the mouse array 1 (MAR1) microarrays that contained the 11,520 clones created above. Following printing, the slides were postprocessed by rehydrating, ultraviolet cross-linking (60 mJ), and then incubating in a blocking solution (335 ml 1-methyl-2-pyrrolidinone into which 6 g succinic anhydride is dissolved followed by 15 ml of 1 mol/l boric acid) for 15 min. Boiling water was used to denature the cDNA on each slide, followed by a brief rinse in 95% ethanol before drying by centrifugation.

Hybridization. Ten micrograms of total splenic RNA (RNeasy Midi Kit, Qiagen) was reverse transcribed to incorporate aminoallyl dUTP (Sigma) into the cDNA for each of the 117 individual mice (Table 1). The reaction was purified (QIAquick PCR Purification Kit, Qiagen), reduced to 5 μ l volume, and then coupled to the monofunctional NHS ester Cy3 (Amersham Biosciences) for 1 h. The reference RNA, a pool of total RNA from 10 NOD and 10 B6 mice at 4 weeks, was processed in the manner described above and labeled with Cy5. The Cy3-labeled sample and Cy5-labeled reference were combined and purified (QIAquick PCR Purification Kit). The combined labeled product plus 15 μ l 20 \times sodium chloride–sodium citrate, 1.8 μ l Cot-1 DNA (0.1 μ g/ μ l), and 2.25 μ l 10% sodium dodecyl sulfate was applied to an MAR1 microarray and incubated at 65°C for 16 h. The arrays were washed briefly and then scanned using the Affymetrix 418 Scanner (MWG Biotech). Each of the 117 samples was compared with our reference using the MAR1 microarrays.

Data analysis. MolecularWare (Cambridge, MA) and ScanAlyze programs were used to extract intensity values from the individual spots. The extracted data were flagged (13) and then uploaded into Another Microarray Database (AMAD), where the normalized intensity values were calculated for each array during submission. The data were extracted and divided into biologically relevant groups for analysis using a nonparametric Mann-Whitney *U* test (Statistica) to identify those genes that can best distinguish the groups. Hierarchical clustering was used to cluster genes with the similarity metric correlation (uncentered) and average linkage clustering in the Cluster program. The results were then viewed using TreeView.

Real-time PCR. Reverse transcription (RT) was performed from 3 μ g total RNA from an independent set of 8 3-week, 10 6-week, and 11 10 week NOD mice using 2 μ l poly T primer and sufficient diethyl pyrocarbonate (DEPC) water to total 10 μ l. The RT reactions were placed at 70°C for 10 min and then on ice for 5 min. The following were added to each reaction and put into a thermocycler (MJ Research) at 42°C for 2 h before being diluted 1:1 with purified water: 1 μ l 10 mmol/l dNTP, 2 μ l 10 \times RT buffer, 1.5 μ l RT enzyme (Stratagene), and 5.5 μ l DEPC water. A control RNA pool was created (30 NOD samples above in equal amounts) and run as an internal control at the following dilutions: 1:1, 1:4, and 1:8. Each of the sample and control RT dilutions were set up in triplicate for real-time PCR analysis with 2 μ l diluted RT, 2 μ l 10 \times PCR buffer, 2 μ l 10 mmol/l dNTP, 0.3 μ l forward and reverse primer (20 pmol/ μ l), 0.5 μ l SYBR green, 0.2 μ l FDC, 0.13 μ l *Taq* enzyme, and 12.37 μ l water. Using the iCycler (BioRad), 35 cycles of 94°C for 30 s, 58°C for 30 s, and 72°C for 30 s were performed. PCR yields at the cycle threshold were calculated based on the standard curve. Twelve genes were investigated: *Igf*, *Igh-6*, *B2m*, *Ddx5*, *Fech*, *Car2*, *Ms4a4b*, *Irf4*, *Rab1*, *Cd24a*, *Rik2610305D13*, and *Rik2310075C2*. To normalize each gene, β -actin was amplified for each RNA sample.

RESULTS

Subtractive cDNA library and microarray design. To identify differentially expressed genes in immune tissues, a spleen cDNA library was created using a subtractive approach. Spleen RNA samples from the B6 and NOD mice were used to reduce the representation of abundant and common genes between NOD and B6 mice in such a way that genes with higher expression in the NOD than in the B6 mouse are enriched. However, this approach is unlikely to identify genes with weaker expression in NOD than in

B6 mice. We elected to focus on the genes with higher expression in the NOD mouse because the autoimmune process is expected to induce hyperproliferation and activation of lymphocytes, leading to higher expression of a number of genes. From this library, 11,520 clones were selected, and the inserts were amplified to create the MAR1, which was used throughout this study.

Rapid switch of gene expression near 5 weeks of age in NOD mice. We profiled the expression of 11,520 clones from a splenic cDNA library in 61 NOD mice ranging in age from 1 to 10 weeks. Table 1 presents the number of mice analyzed for each time point and strain. Hierarchical clustering analysis of the complete clone set identified two major groups of mice: immature (1–4 weeks) and mature (6–10 weeks). Over 1,000 clones exhibited differential expression patterns between the two groups of NOD mice. These clones were sequenced and BLAST (basic local alignment search tool) analysis revealed 362 unique genes. The nonparametric Mann-Whitney *U* test was then applied to this unique gene dataset, and 80 genes with known function were significantly different between the immature and mature NOD mice, with a *P* value of $<10^{-4}$ (Fig. 1). Analysis of the 5-week-old NOD mice indicated that they have the immature expression profiles (Fig. 1).

The mean expression levels for the 80 genes in immature NOD mice (group 1) and mature NOD mice (group 2) are presented in Table 2. Please note that the expression levels have been normalized to the immature NOD group. Of the 80 differentially expressed genes, 62 have higher and 18 have lower expression levels in mature NOD compared with immature NOD mice. A number of the genes are lymphoid-specific, and many are involved in the normal cellular processes such as transcription, translation, DNA replication, signal transduction, and apoptosis. **Confirmation of differential expression by real-time PCR.** Real-time PCR was used to confirm the expression differences revealed by the microarray technique. We included nine genes that have a *P* value of $<5 \times 10^{-5}$: immunoglobulin joining chain (*Igf*), immunoglobulin heavy chain 6 (*Igh-6*), β -2-microglobulin (*B2m*), DEAD box polypeptide 5 (*Ddx5*), ferrochelatase (*Fech*), carbonic anhydrase 2 (*Car2*), membrane-spanning 4-domains, subfamily A, member 4B (*Ms4a4b*), interferon regulatory factor 4 (*Irf4*), and *CD24a*. We also included two genes that showed differences but did not quite reach our stringent statistical criterion: RAB1 member of the RAS oncogene family (*Rab1*) (*P* = 0.0008) and Riken cDNA 2310075C12 (*Rik231*) (*P* = 0.0001). Finally, the Riken cDNA 2610305D13 clone (*Rik261*), which had a 3.8-fold difference by microarray, was analyzed by real-time RT-PCR even though it was not highly significant (*P* = 0.02). Splenic total RNA samples from 8 NOD mice at 3 weeks, 10 NOD mice at 6 weeks, and 11 NOD mice at 10 weeks were isolated and analyzed for these 12 genes (Table 3). Real-time PCR was able to confirm the microarray expression differences for all nine genes that have highly significant differences between immature and mature NOD mice. Real-time PCR was also able to confirm that *Rik261* was not different between immature and mature NOD mice. However, the real-time PCR and microarray data disagreed for the two genes, *Rab1* and *Rik231*, that did not reach the stringent statistical threshold. Indeed, the real-

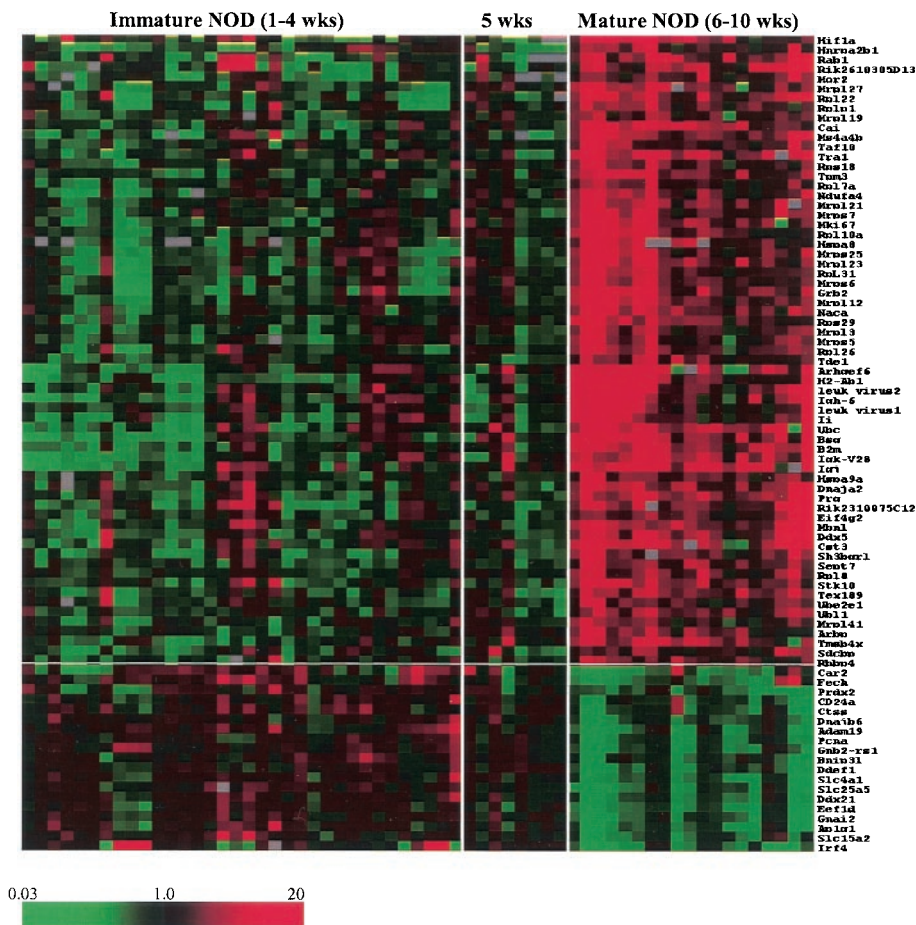


FIG. 1. Novel temporal transition in NOD mice between 5 and 6 weeks of age. Expression profiles of significantly different genes ($P > 10^{-4}$) between immature (1–4 weeks) and mature (6–10 weeks) NOD mice, with the columns representing individual mice and the rows corresponding to the gene indicated in the right-hand column. Green indicates the expression level is lower than that in the common reference, while red indicates an expression level that is higher than the common reference. The bar indicates the fold difference.

time PCR data were significantly different from the microarray data. The discrepancies between the real-time PCR and microarray data are most likely due to the low intensities on the microarrays for these two genes.

Gene expression changes associated with disease progression and maturation of lymphocytes. The switch in gene expression profiles around 5 weeks of age in NOD mice may be the result of two confounding biological processes: the progression to autoimmunity and the maturation of splenic cells. To dissect these two processes, we analyzed two NOD congenic strains that have little or no incidence of insulinitis or diabetes: NOD.Idd3/Idd10 and NOD.B10Sn-H2^b (<1 and 0% incidence of diabetes, respectively). These mice were chosen as controls instead of B6 because they have the NOD background. Any differences seen are more likely to be due to the disease process than to strain differences. Figure 2 displays the expression profiles of the 56 congenic NOD mice for the 80 genes differentially expressed between immature and mature NOD. Interestingly, many of the genes also exhibit a similar temporal change in the congenic mice (Fig. 2A). Fifteen of the 80 genes did not show the same trend of temporal changes in NOD congenic mice (Fig. 2B). These 15 genes exhibiting temporal changes in NOD but not in NOD congenic mice are in boldface in Table 2 (compare the P values for immature and mature NOD [group 1 vs. 2] with the immature and mature NOD congenics [group 3 vs. 4]). These genes do not fall within one functional category, but are distributed across multiple functional groups. One of the genes,

hypoxia inducible factor-1 α (*Hif1a*), is upregulated in the NOD and downregulated in the NOD congenic mice.

Expression levels in immature NOD versus congenic NOD mice. To identify those genes that are different in the preinsulinitis stage, the mean expression levels in the immature NOD (group 1) and the immature congenic (group 3) mice for the 80 genes were compared (1 vs. 3 in Table 2). The vast majority of the genes are not different between these two groups of mice. Twelve genes displayed a trend of lower expression in NOD when compared to the congenic mice ($P < 0.05$). Six of the 12 genes (*Bsg*, *B2m*, *Ii*, *Igh-6*, *Igk-V28*, and *Igj*) are lymphoid-specific and expressed in antigen-presenting cells. Among the 12 genes, only the *Hif1a* gene has a 1.8-fold higher expression in the congenics than the NOD with a reasonable P value (0.0008). Other confirmatory tests will need to be performed to determine whether any of these genes are truly different between the NOD and congenic NOD mice before the onset of insulinitis.

Expression differences between mature NOD and congenic NOD mice. Of the 80 genes that showed temporal changes in the NOD mice, 56 have a higher expression level in the mature NOD than the mature NOD congenic mice (Table 2, group 2 vs. 4). This increase is significant for 19 of the genes ($0.001 < P < 0.05$) and highly significant for 10 other genes ($P < 0.001$). These latter genes are involved in MHC class II processing (*Hspa8*), B-cell development, apoptosis control (*Hif1a*), transcription (*Hnrpa2b1* and *Taf10*), translation (*Eif4g2*), and protein transport (*Dnaja2*). These data are consistent

TABLE 2
Summary of average relative expression data with corresponding *P* values

Gene	Description	Groups				<i>P</i> value			
		1 NOD _{Imm}	2 NOD _{Mat}	3 Cong _{Imm}	4 Cong _{Mat}	1 vs. 2	3 vs. 4	1 vs. 3	2 vs. 4
Lymphocyte specific									
<i>Stk10</i>	Differentiation and activation pathways	1	2.6	1.1	2.4	4 E-06	0.0003	NS	NS
<i>Ms4a4b*</i>	Expressed on Th1 not Th2 T-cells (integral membrane protein)	1	2.5	1.1	2.2	2 E-05	5 E-05	NS	NS
<i>Tmsb4x</i>	Cytoskeleton actin binding	1	3.9	1.2	2.6	<1 E-07	2 E-06	NS	0.005
<i>Bsg</i>	T-cell maturation (membrane protein)	1	4.9	1.4	3.5	<1 E-07	1 E-07	0.02	0.04
<i>Irf4*</i>	Transcription factor (expressed only in lymphoid cells)	1	0.3	0.4	0.6	4 E-05	NS	0.005	0.006
APC specific									
MHC class I processing									
<i>Tra1</i>	Chaperones proteins to MHC class I (DC maturation)	1	3.0	1.4	2.3	2 E-06	0.007	NS	0.03
<i>B2m*</i>	MHC class I, implicated as <i>Idd13</i> susceptibility gene	1	3.4	1.2	2.6	<1 E-07	<1 E-07	0.05	NS
MHC class II processing									
<i>Hspa8</i>	Binds Ii	1	2.4	1.0	1.0	0.0001	NS	NS	0.0001
<i>Ii</i>	MHC class II processing	1	2.9	1.4	2.5	2 E-06	3 E-06	0.007	NS
<i>Ctss</i>	Key enzyme for Ii degradation (MHC class II)	1	0.5	1.2	0.4	3 E-05	<1 E-07	NS	NS
<i>H2-Ab1</i>	Antigen presentation, exogenous antigen defense response	1	2.8	1.0	2.3	3 E-05	<1 E-07	NS	NS
B-cell specific									
<i>Sdcbp</i>	B-cell development (binds Sox4 to IL5Ralpha)	1	1.8	1.0	1.3	0.0002	0.01	NS	0.01
<i>Igh-6*</i>	Heavy chain of IgM	1	3.2	1.3	2.6	<1 E-07	<1 E-07	0.004	0.04
<i>Igk-V28</i>	Humoral immune response	1	4.2	1.3	3.4	<1 E-07	<1 E-07	0.02	NS
<i>Igi*</i>	Humoral immune response	1	3.8	1.4	3.1	<1 E-07	2 E-05	0.007	NS
<i>CD24a*</i>	Activation and differentiation of B-cells	1	0.5	1.1	0.5	4 E-06	<1 E-07	NS	NS
Signal transduction									
<i>Gnb2-rs1</i>	Adaptor protein in INFa and IL-5/IL-3/GMCSF-R signaling	1	0.4	0.9	0.7	<1 E-07	0.02	NS	0.02
<i>Hspa9a</i>	Stress response, intracellular trafficking, antigen processing	1	1.9	1.0	1.3	0.0004	0.004	NS	0.005
<i>Grb2</i>	Intracellular signaling in B-cells and T-cells	1	3.8	1.1	2.5	2 E-06	2 E-06	NS	0.03
<i>Gnai2</i>	Transmembrane signaling	1	0.4	1.1	0.4	<1 E-07	<1 E-07	NS	NS
<i>Arhgef6</i>	Involved in activation of Rho proteins	1	3.7	1.3	3.7	1 E-05	<1 E-07	NS	NS
Apoptosis									
<i>Hif1a</i>	Transcription factor (B-cell development, apoptosis control)	1	2.3	1.8	0.9	0.0009	2 E-06	0.0008	0.0002
<i>Ubl1</i>	Protection against apoptosis, inhibits NF-κB signal transduction	1	2.3	1.1	1.6	7 E-06	0.005	NS	0.04
<i>Bnip31</i>	Induce apoptosis (located in mitochondria)	1	0.6	1.0	0.8	<1 E-07	4 E-05	NS	NS
<i>Prdx2</i>	Apoptosis inhibitor (response to oxidative stress)	1	0.5	1.0	0.5	2 E-05	1 E-06	NS	NS

Continued on following page

TABLE 2—Continued

Gene	Description	Groups				P value			
		1 NOD _{Imm}	2 NOD _{Mat}	3 Cong _{Imm}	4 Cong _{Mat}	1 vs. 2	3 vs. 4	1 vs. 3	2 vs. 4
Cell proliferation									
<i>Mki67</i>	Required for cell proliferation	1	3.1	1.2	1.9	<1 E-07	0.0003	NS	0.001
<i>Ddx5*</i>	Proliferation-associated nuclear antigen	1	3.0	1.1	2.1	<1 E-07	3 E-06	NS	0.007
Cytoskeleton/ cytokinesis									
<i>Ddef1</i>	Cytoskeletal regulation and cell motility	1	0.5	0.9	0.7	4 E-06	NS	NS	0.02
<i>Sept7</i>	Cytokinesis	1	2.4	1.2	2.0	2 E-06	3 E-05	NS	NS
<i>Tpm3</i>	Cytoskeleton, actin binding, muscle development	1	2.6	0.9	1.8	<1 E-07	7 E-05	NS	0.02
DNA replication									
<i>Pcna</i>	Regulation of DNA replication	1	0.4	0.8	0.7	1 E-06	NS	0.004	0.02
<i>Rbbp4</i>	Mediates chromatin assembly in DNA replication and DNA repair	1	1.9	0.7	1.2	6 E-05	6 E-05	0.002	0.001
Membrane proteins									
<i>Tde1</i>	Plasma membrane	1	2.0	1.1	1.3	1 E-06	NS	NS	0.0006
<i>Prg</i>	Protein core of membrane protein	1	2.6	1.3	2.0	1 E-06	0.005	0.03	0.05
<i>Adam19</i>	Proteolytic processing (DC differentiation)	1	0.4	1.0	0.6	5 E-06	8 E-05	NS	NS
<i>Slc15a2</i>	Transport of small peptides (membrane protein)	1	0.5	1.2	0.6	9 E-05	3 E-05	NS	NS
<i>Slc4a1</i>	Glucose and anion transport (glucose transport in leukocytes)	1	0.4	1.2	0.5	<1 E-07	<1 E-07	NS	NS
<i>Slc25a5</i>	Facilitates exchange of ADP and ATP btwn mito and cytosol	1	0.3	1.2	0.5	<1 E-07	<1 E-07	0.03	NS
Protein degradation									
<i>Ube2e1</i>	Attaches ubiquitin to proteins	1	2.0	1.1	1.2	0.0005	NS	NS	0.0008
<i>Ubc</i>	Protein degradation	1	3.3	1.3	2.1	3 E-06	0.0008	NS	0.0004
Protein folding, regulation, and transport									
<i>Dnaja2</i>	Co-chaperone to Hsp70	1	2.9	1.3	1.7	2 E-05	0.02	NS	0.003
<i>Dnajb6</i>	Co-chaperone to Hsp70	1	0.6	1.0	0.8	2 E-06	0.0008	NS	NS
<i>Naca</i>	Binds newly synthesized peptides (may complex with Hsp70)	1	2.7	1.1	1.6	<1 E-07	1 E-05	NS	0.0002
<i>Cai</i>	Protein folding	1	3.1	1.2	2.1	2 E-06	1 E-05	NS	0.01
<i>Ap1g1</i>	Protein transport (from golgi)	1	0.4	1.2	0.4	1 E-06	<1 E-07	NS	NS
<i>Cst3</i>	Protein regulation	1	2.9	1.2	2.5	<1 E-07	<1 E-07	NS	NS
Ribosomal biogenesis									
<i>Rps18</i>	Ribosome biogenesis	1	2.1	1.3	1.9	5 E-05	0.002	0.04	NS
<i>Rpl26</i>	Ribosome biogenesis	1	2.3	1.1	1.7	6 E-06	0.003	NS	0.04
<i>Rps29</i>	Ribosome biogenesis, protein biosynthesis	1	2.7	1.1	1.8	1 E-06	0.0001	NS	0.03
<i>Mrpl41</i>	Ribosome biogenesis	1	1.9	1.0	1.5	0.0001	7 E-05	NS	NS
<i>Rpl22</i>	Ribosome biogenesis	1	3.4	1.3	2.5	2 E-05	2 E-05	NS	NS
<i>Idx21</i>	Ribosomal RNA biogenesis and transcription	1	0.4	1.2	0.5	<1 E-07	<1 E-07	NS	NS
Routine cell functions									
<i>Mor2</i>	Enzyme in citric acid cycle	1	2.0	1.0	2.0	0.0001	0.0003	NS	NS

Continued on following page

TABLE 2—Continued

Gene	Description	Groups				P value			
		1 NOD _{Imm}	2 NOD _{Mat}	3 Cong _{Imm}	4 Cong _{Mat}	1 vs. 2	3 vs. 4	1 vs. 3	2 vs. 4
<i>Ndufa4</i>	First enzyme in electron transport chain	1	2.4	1.0	1.9	0.0005	7 E-05	NS	NS
<i>Car2*</i>	Reversible hydration of carbon dioxide	1	0.5	1.3	0.5	1 E-05	1 E-06	0.03	NS
<i>Fech*</i>	Heme and porphyrin biosynthesis	1	0.6	1.1	0.6	6 E-06	<1 E-07	NS	NS
Transcription									
<i>Hnrpa2b1</i>	Transcription regulation	1	2.1	0.9	1.0	1 E-05	NS	NS	3 E-06
<i>Taf10</i>	Transcription	1	2.4	1.0	1.2	2 E-05	0.03	NS	7 E-05
<i>Tex189</i>	Chromatin modeling, transcriptional regulator	1	2.7	1.0	2.0	3 E-06	2 E-06	NS	0.02
Translation									
<i>Mrp119</i>	Protein biosynthesis	1	1.7	1.5	1.8	0.0008	NS	0.0001	NS
<i>Eif4g2</i>	Translation (role in INFγ-induced apoptosis?)	1	1.8	1.2	1.6	9 E-05	0.04	NS	NS
<i>Mrpl27</i>	Protein biosynthesis	1	3.2	1.5	2.2	<1 E-07	0.003	0.002	0.02
<i>Mrps5</i>	Protein biosynthesis	1	1.9	1.1	1.4	3 E-05	0.004	NS	0.03
<i>Rpl31</i>	Protein biosynthesis	1	2.4	1.2	1.6	<1 E-07	0.008	NS	0.0008
<i>Rpl8</i>	Protein biosynthesis	1	2.0	1.1	1.6	2 E-05	0.0004	NS	NS
<i>Rplp1</i>	Translational elongation	1	3.2	1.2	2.2	2 E-06	0.0004	NS	0.02
<i>Mrps7</i>	Protein biosynthesis	1	2.5	1.1	1.6	1 E-06	0.0003	NS	0.004
<i>Mrpl3</i>	Protein biosynthesis	1	1.9	1.0	1.5	0.0002	0.0006	NS	0.01
<i>Rpl7a</i>	Protein biosynthesis	1	1.7	1.0	1.7	1 E-05	4 E-06	NS	NS
<i>Mrpl23</i>	Protein biosynthesis	1	2.8	1.2	1.8	<1 E-07	7 E-05	NS	0.001
<i>Rpl10a</i>	Protein biosynthesis	1	2.3	0.9	1.7	<1 E-07	3 E-05	NS	0.03
<i>Mrpl12</i>	Protein biosynthesis	1	3.0	1.1	2.0	<1 E-07	7 E-05	NS	0
<i>Mrps25</i>	Mitochondrial small ribosomal subunit	1	2.7	1.1	2.0	<1 E-07	2 E-05	NS	0.02
<i>Mrps6</i>	Protein biosynthesis	1	2.9	1.1	2.0	<1 E-07	3 E-06	NS	0.008
<i>Mrpl21</i>	Protein biosynthesis	1	2.4	1.1	1.7	<1 E-07	1 E-05	NS	0.002
<i>Arbp</i>	Protein biosynthesis, translational elongation	1	2.1	1.0	1.6	1 E-06	<1 E-07	NS	NS
<i>Eef1d</i>	Protein biosynthesis	1	0.4	1.2	0.4	<1 E-07	<1 E-07	NS	NS
Unkown									
Leuk virus 2	Not known	1	2.9	1.1	1.2	3 E-05	NS	NS	0.0008
Leuk virus 1	Not known	1	2.2	1.3	1.3	0.0004	NS	0.01	0.04
<i>nbn1</i>	dsRNA binding	1	2.4	1.2	1.5	<1 E-07	0.002	NS	0.003
<i>Sh3bgrl</i>	Not known	1	2.5	0.9	2.1	0.0004	0.001	NS	NS
<i>Rik2610305D13*</i>	Not known	1	3.8	2.6	2.6	0.02	NS	0.01	NS
Real-time data does not agree with microarray data									
<i>Rab1*</i>	Transport of proteins from ER to golgi	1	2.3	1.4	1.4	0.0008	NS	0.04	0.01
<i>Rik2310075C12*</i>	Not known	1	1.9	1.7	2.0	9 E-05	NS	0.008	NS

Bold, genes significantly different between the immature and mature NOD mice but not significantly different in the NOD congenic mice. Note: All expression levels have been normalized to the immature NOD mice. DC, dendritic cell; ER, endoplasmic reticulum; NS, not significant. *Real-time data have been collected for this gene.

with the hyperactivated state of lymphocytes in the NOD mouse at the time of ongoing autoimmunity.

DISCUSSION

Because of its complex nature, it is a challenging task to understand the immunopathogenesis of type 1 diabetes. Since the identification of a spontaneous mouse model (NOD) two decades ago (14), our knowledge about the key players involved in type 1 diabetes has expanded exponentially. However, the underlying molecular mechanism of each of these key players and how they function together

to create the disease phenotype remains elusive. The development of microarray technology has provided a new approach to understanding diabetes pathogenesis through the analysis of global gene expression profiles. In this study, we used microarrays to monitor the global splenic gene expression of NOD and NOD congenic mice, ages 1–10 weeks. The purpose of this experiment was to gain a better understanding of the molecular events that occur in the immune system of the NOD mouse during the development of insulinitis [the infiltration of lymphocytes into the pancreatic islets that begins around 3 weeks (15)], but

TABLE 3
Real-time results compared to microarray results

Gene	Real-time RT-PCR					Microarray	
	ΔC_T 3 weeks (n = 8)	ΔC_T 6-10 weeks (n = 21)	$\Delta\Delta C_T$	Fold change (6-10 weeks/3 weeks)	P value	Fold change (6-10 weeks/3 weeks)	P value
Agreement							
<i>Igj</i>	5.5 ± 0.4	3.7 ± 1.2	1.9	3.6	0.0005	3.8	<10 ⁻⁷
<i>B2m</i>	0.4 ± 0.3	-0.7 ± 0.5	1.1	2.1	0.00004	3.4	<10 ⁻⁷
<i>Igh-6</i>	0.5 ± 0.3	-0.4 ± 0.6	0.9	1.9	0.001	3.2	<10 ⁻⁷
<i>Cd24a</i>	5.2 ± 0.3	7.6 ± 0.9	-2.4	0.2	0.00004	0.5	4 × 10 ⁻⁶
<i>Ddx5</i>	1.4 ± 0.2	0.5 ± 0.5	0.8	1.8	0.00007	3.0	<10 ⁻⁷
<i>Car2</i>	-0.1 ± 0.6	2.4 ± 1.3	-2.5	0.2	0.00007	0.5	<10 ⁻⁵
<i>Fech</i>	2.1 ± 0.4	4.6 ± 1.1	-2.5	0.2	0.00004	0.6	6 × 10 ⁻⁶
<i>Ms4a4b</i>	9.1 ± 0.6	7.0 ± 0.6	2.1	4.2	0.00005	2.5	2 × 10 ⁻⁵
<i>Irf4</i>	11.5 ± 0.2	11.8 ± 0.4	-0.3	0.8	0.01	0.3	4 × 10 ⁻⁵
<i>Rik261</i>	5.8 ± 0.6	5.5 ± 0.9	0.3	1.2	NS	3.8	0.02 (NS)
Nonagreement							
<i>Rab1</i>	9.4 ± 0.4	9.9 ± 0.4	-0.5	0.7	0.02	2.3	0.0008
<i>Rik231</i>	8.8 ± 0.5	9.9 ± 0.5	-1.1	0.5	0.00008	1.9	0.0001

Data are means ± SD unless otherwise indicated. Each sample was run in triplicate, then normalized by subtracting the median C_T of β -actin from the median C_T of each sample. The ΔC_T for each group was calculated by averaging the C_T for each group (3 weeks and 6-10 weeks). $\Delta\Delta C_T = \Delta C_T$ 3 weeks - ΔC_T 6-10 weeks. The P value was calculated using the nonparametric Mann-Whitney U test. The fold difference for the real-time data was calculated as follows: $2^{\Delta\Delta C_T}$. The microarray data comes from Table 2. C_T , cycle threshold; NS, not significant.

before the onset of overt diabetes. Because our microarray experiments analyzed the expression of over 10,000 clones simultaneously, a large number of genes may show differences due to random chance. Therefore, a stringent statistical threshold and appropriate gene selection method

must be used to reduce the false-positive rate. In this study, we have generated real-time PCR data for a small number of genes selected based on the microarray data in order to select the most appropriate statistical methods for gene selection and establish the appropriate statistical

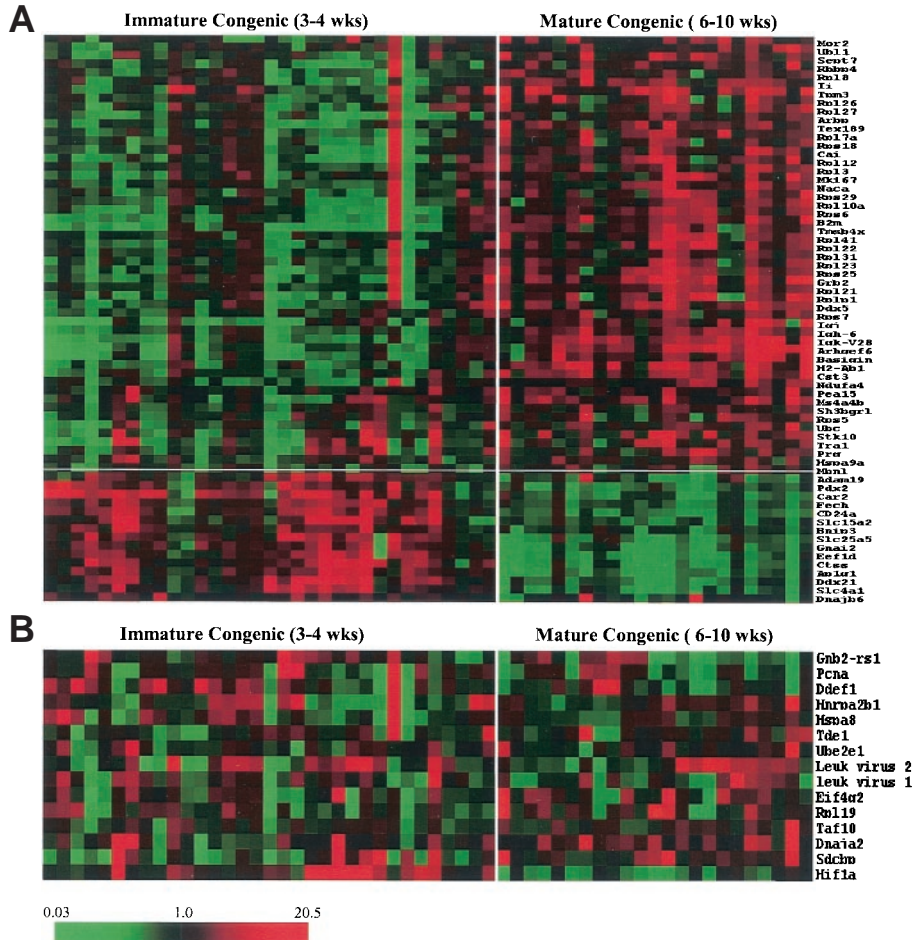


FIG. 2. Expression profiles of two NOD congenic mouse strains, NOD.Idd3/Idd10 and NOD.B10Sn-H2b, from 3 to 10 weeks of age. **A**: Profiles of the 65 genes that reflect the same transition between 3-4 and 6-10 weeks seen in the NOD mice. **B**: Profiles of the 15 genes that do not change temporally in the NOD congenic mice, but do in the NOD mice. Columns represent individual mice, while rows correspond to the gene indicated in the right-hand column. Green indicates the expression level is lower than that in the common reference, while red indicates an expression level that is higher than the common reference. The bar indicates the fold difference.

threshold. The Mann-Whitney U test coupled with the statistical threshold of $P < 5 \times 10^{-5}$ seems to be the best compromise between higher sensitivity and lower false-positive rate. When this is applied to our microarray dataset, 100% of the genes tested by real-time PCR are concordant with the microarray data. Genes with a $P > 5 \times 10^{-5}$ may be considered, but the false-positive rate will increase at higher values. This should be kept in mind when interpreting any microarray data.

Our microarray dataset can be used to address several questions for autoimmune diabetes. The first question relates to the temporal changes of gene expression in NOD mice. Analysis of 61 NOD (1–10 weeks) splenic profiles revealed many genes rapidly changing expression levels between 5 and 6 weeks of age. This switch of gene expression defined two distinct groups of mice: immature (1–4 weeks) and mature (6–10 weeks). Among the top 80 differentially expressed genes, 62 had increased levels of expression in the mature NOD mice. These genes fall into a broad range of functional groups. The largest expression increases occurred in lymphoid-specific genes, suggesting that the splenic immune cells have increased cellular activities beginning around the 6-week time point. Specifically, significant increases were seen in B-cell genes such as *Igj*, *Igk-V28*, and *Igh-6*, suggesting higher antibody production. Increased antigen presentation is suggested by increased expression of MHC class I and class II antigen processing genes (*Tra1*, *Hspa8*, *Hspa9a*, *Ii*, and *H2-Ab1*) and β 2-microglobulin (*B2m*). Interestingly, only a few T-cell-related genes (*Ms4a4b* and *Bsg*) are increased in the mature NOD mice. Several upregulated genes are involved in cell proliferation (*Mki67* and *Ddx5*) and signal transduction in lymphocytes (*Gnb2-rs1*, *Grb2*, and *Gnai2*), suggesting increased lymphocyte proliferation and activation. Several genes (*Hif1a*, *Ubl1*, *Bnip3l*, *Prdx2*) are implicated in apoptosis control. Also, a large number of genes are related to basic cellular activities, which is not surprising given the higher proliferation and activation of splenocytes. These findings are consistent with the ongoing autoimmune response when NOD mice progress to invasive insulinitis by 8–10 weeks of age (15). Our data suggest that an active autoimmune response is well underway by 6 weeks of age in the NOD.

The discovery of the rapid transition from immature to mature phenotype in the NOD spleens has significant implications for future research and may help explain the results from diabetes prevention studies. For example, administration of linomide (16), recombinant human interleukin-13 (17), or insulin (18–21) to 4- to 5-week-old NOD mice has been shown to significantly delay or prevent diabetes, along with a long list of other treatments (22). However, administration of one of these three substances to “mature” NOD mice is less effective. In light of our results, the mechanisms of action of linomide, human interleukin-13, and insulin could modulate the splenic immune cells, delaying or preventing the change that occurs at 6 weeks and thus delaying or preventing the onset of diabetes. This would explain why treatment after the 6-week transition results in reduced efficacy of the treatments.

Analysis of the two NOD congenic strains with near zero incidences of insulinitis and diabetes, NOD.Idd3/Idd10 and

NOD.B10Sn-H2^b, is critical to understanding the microarray data. Interestingly, the majority of the temporal changes observed in NOD mice also occur in the NOD congenic mice (Table 2). These results are not surprising given that many of the changes may be related to the normal development of the immune system. However, 15 genes were significantly different in the immature versus mature NOD mice but not significantly different between immature and mature NOD congenic mice (Fig. 2B and boldfaced genes in Table 2). Four of these genes (*Hspa8*, *Sdcbp*, *Gnb2-rs1*, and *Hif1a*) are lymphoid-specific or function in apoptosis or signal transduction. These genes may play important roles in the pathogenesis of type 1 diabetes.

The comparison between the mature NOD and diabetes-protective NOD congenic mice revealed very interesting findings. First, the vast majority of the genes in Table 2 have higher expression in the mature congenic mice (group 4 in Table 2) than in either immature NOD (group 1) or immature congenic (group 3) mice but lower expression than in the mature NOD mice (group 2). However, the differences between the mature NOD and congenic mice are not statistically significant for most genes. It is tempting to suggest that the propensity of developing type 1 diabetes is due more to quantitative differences than to qualitative differences. Ten genes are significantly different between the two groups at $P < 0.001$. These 10 genes include *Hspa8*, *Hif1a*, and genes involved in basic cellular functions such as transcription. The data, taken together, seem to indicate hyperactivation and proliferation of lymphocytes in the NOD mice with active autoimmunity.

A critical issue for the immunopathogenesis of type 1 diabetes is to identify the key molecules implicated in the initiation of autoimmunity. We attempted to address this question by comparing age-matched NOD and protective congenic mice before or right at the beginning of insulinitis. We only found one gene (*Hif1a*) that is significantly higher in the congenics than in the NOD mice (1.8-fold increase, $P = 0.0008$). Further studies are required to assess the role of *Hif1a*.

Of the 80 genes identified, 7 are located within confirmed diabetes susceptibility regions. Two of the seven genes, β 2-microglobulin (*B2m*) in the *Idd13* region (23,24) and *H2-Ab1* within the *I-A* locus in the *Idd1* interval (25,26), have already been implicated in type 1 diabetes. The five other genes that map to type 1 diabetes susceptibility regions are heat shock protein 8 (*Idd2*), ubiquitin-like 1 (*Idd5*), retinoblastoma binding protein 4 (*Idd9.1*), proliferating cell nuclear antigen (*Idd13*), and interferon regulatory factor 4 (*Idd14*).

The retinoblastoma binding protein 4 (*Rbbp4*) functions as a mediator of chromatin assembly in DNA replication and repair (27). It is universally expressed, and there is no significant difference in expression between the NOD and congenic NOD mice for *Rbbp4* (Table 2); therefore, *Rbbp4* is not a likely candidate gene for type 1 diabetes even though it maps to the *Idd9.1* region.

Heat shock protein 8 (*Hspa8*) has recently been shown to aid in the targeting of the invariant chain/MHC class II complex to endocytic compartments (28). *Hspa8* is upregulated in the NOD mice from 1–4 to 6–10 weeks, but not in the NOD congenic mice (Table 2). The map position,

pattern of differential expression, and function of this gene suggest that it is an ideal candidate gene within the *Idd2* interval.

Ubiquitin-like 1 (*Ubl1*), also known as sentrin, GMP1, SUMO-1, or PIC1, was identified in 1996 by several different groups (29–33). Ubiquitin-like protein 1, NEDD8, and Apg12 are a newly discovered group of ubiquitin-like proteins that are involved in protein modification (34). Okura et al. (30) demonstrated that when *Ubl1* is overexpressed, cells are protected from both anti-Fas/APO-1 and tumor necrosis factor-induced cell death. Ubiquitin-like protein 1 has also been shown to modify I κ B α (35), making it resistant to degradation. Because I κ B α inhibits NF- κ B, an increase in ubiquitin-like protein 1 could decrease the expression of genes controlled by NF- κ B, including genes involved in immune and inflammatory responses. Thus, overexpression of *Ubl1* in a specific subset of splenic cells could indicate resistance to apoptosis or a decrease in immune response, both of which could significantly affect the pathogenesis of type 1 diabetes. Although *Ubl1* is increasing in both the NOD and congenic NOD mice, it appears to have a higher expression level in the mature NOD mice (Table 2, group 2 vs. 4, $P = 0.04$) making it a good candidate gene for *Idd5*.

Interferon regulatory factor 4 (*Irf4*) is a lymphocyte-specific transcription factor involved in B- and T-cell function (36,37). The immature NOD mouse has the highest expression when compared with both the mature NOD and immature and mature congenic NOD mouse. The real-time data (Table 3) confirm that the immature NOD mouse has a higher expression than the mature NOD mouse. The location of *Irf4* within a diabetes susceptibility region, its immune function, and its differential expression in NOD versus congenic NOD mice make *Irf4* another excellent candidate gene for type 1 diabetes.

In summary, our studies have revealed a number of genes that are differentially expressed between NOD and NOD congenic mice at various time points. Some of these genes may play critical roles in the initiation and progression of type 1 diabetes. Two of the 80 genes exhibiting differential expression have previously been implicated in type 1 diabetes. Our study revealed another three excellent candidate genes, *Hspa8* (*Idd2*), *Ubl1* (*Idd5*), and *Irf4* (*Idd14*). The data also allowed us to define a critical checkpoint (around 5 weeks) during the development of autoimmune diabetes in NOD mice. This checkpoint is marked by the maturation/activation of lymphocytes and a massive switch of gene expression. Detailed analysis of the molecular events in individual cell types occurring at the checkpoint should further shed light on the pathogenesis of the disease.

ACKNOWLEDGMENTS

We gratefully acknowledge Dr. Mark Yang and Dr. James Yang from the University of Florida for their help with the statistical programs used in our data analysis and Dr. Ed Leiter from The Jackson Laboratory for generously providing the NOD.Idd3/Idd10 breeders. Funding was provided by a National Institute of Diabetes and Digestive and Kidney Diseases biotechnology center grant (NIH 5 U24 DK58778-02) and project 1 of program project 2P01 AI-42288-05 from the National Institutes of Health.

REFERENCES

- Serreze DV, Chapman HD, Varnum DS, Hanson MS, Reifsnnyder PC, Richard SD, Fleming SA, Leiter EH, Shultz LD: B lymphocytes are essential for the initiation of T cell-mediated autoimmune diabetes: analysis of a new "speed congenic" stock of NOD.Ig mu null mice. *J Exp Med* 184:2049–2053, 1996
- Akashi T, Nagafuchi S, Anzai K, Kondo S, Kitamura D, Wakana S, Ono J, Kikuchi M, Niho Y, Watanabe T: Direct evidence for the contribution of B cells to the progression of insulinitis and the development of diabetes in non-obese diabetic mice. *Int Immunol* 9:1159–1164, 1997
- Noorchashm H, Noorchashm N, Kern J, Rostami SY, Barker CF, Najj A: B-cells are required for the initiation of insulinitis and sialitis in nonobese diabetic mice. *Diabetes* 46:941–946, 1997
- Christianson SW, Shultz LD, Leiter EH: Adoptive transfer of diabetes into immunodeficient NOD-scid/scid mice: relative contributions of CD4+ and CD8+ T-cells from diabetic versus prediabetic NOD.NON-Thy-1a donors. *Diabetes* 42:44–55, 1993
- Bendelac A, Carnaud C, Boitard C, Bach JF: Syngeneic transfer of autoimmune diabetes from diabetic NOD mice to healthy neonates: requirement for both L3T4+ and Lyt-2+ T cells. *J Exp Med* 166:823–832, 1987
- Yoon JW, Jun HS: Cellular and molecular pathogenic mechanisms of insulin-dependent diabetes mellitus. *Ann N Y Acad Sci* 928:200–211, 2001
- Rieneck K, Bovin LF, Josefsen K, Buschard K, Svenson M, Bendtzen K: Massive parallel gene expression profiling of RINm5F pancreatic islet beta-cells stimulated with interleukin-1beta. *APMIS* 108:855–872, 2000
- Cardozo AK, Kruhoffer M, Leeman R, Orntoft T, Eizirik DL: Identification of novel cytokine-induced genes in pancreatic β -cells by high-density oligonucleotide arrays. *Diabetes* 50:909–920, 2001
- Shalev A, Pise-Masison CA, Radonovich M, Hoffmann SC, Hirshberg B, Brady JN, Harlan DM: Oligonucleotide microarray analysis of intact human pancreatic islets: identification of glucose-responsive genes and a highly regulated TGFbeta signaling pathway. *Endocrinology* 143:3695–3698, 2002
- She JX, Eckenrode S, Ruan QG, Marron MP, Li QZ, Yang MCK, Yang J, Hopkins D, Muir A, McIndoe RA: Microarray technology in the pathogenesis and management of autoimmune disorders. In *New Concepts in Pathology and Treatment of Autoimmune Disorders*. Pozzilli P, Pozzilli C, Kapp JF, Eds. New York, Springer-Verlag, 2001, p. 1–14
- Eaves IA, Wicker LS, Ghandour G, Lyons PA, Peterson LB, Todd JA, Glynn RJ: Combining mouse congenic strains and microarray gene expression analyses to study a complex trait: the NOD model of type 1 diabetes. *Genome Res* 12:232–243, 2002
- Diatchenko L, Lau YFC, Campbell AP, Chenchik A, Moqadam F, Huang B, Lukyanov S, Lukyanov K, Gurskaya N, Sverdlov ED, Siebert PD: Suppression subtractive hybridization: a method for generating differentially regulated or tissue-specific cDNA probes and libraries. *Proc Natl Acad Sci U S A* 93:6025–6030, 1996
- Yang MC, Ruan QG, Yang JJ, Eckenrode S, Wu S, McIndoe RA, She JX: A statistical method for flagging weak spots improves normalization and ratio estimates in microarrays. *Physiol Genomics* 7:45–53, 2001
- Makino S, Kunimoto K, Muraoka Y, Mizushima Y, Katagiri K, Tochino Y: Breeding of a non-obese, diabetic strain of mice. *Jikken Dobutsu* 29:1–13, 1980
- Bach JF: The natural history of islet-specific autoimmunity in NOD mice. In *NOD Mice and Related Strains: Research Applications in Diabetes, AIDS, Cancer and Other Diseases*. Leiter EH, Atkinson M, Eds. New York, R.G. Landes, 1998, p. 121–144
- Gross DJ, Sidi H, Weiss L, Kalland T, Rosenmann E, Slavov S: Prevention of diabetes mellitus in non-obese diabetic mice by linomide, a novel immunomodulating drug. *Diabetologia* 37:1195–1201, 1994
- Zaccane P, Phillips J, Conget I, Gomis R, Haskins K, Minty A, Bendtzen K, Cooke A, Nicoletti F: Interleukin-13 prevents autoimmune diabetes in NOD mice. *Diabetes* 48:1522–1528, 1999
- Atkinson MA, Maclaren NK, Luchetta R: Insulinitis and diabetes in NOD mice reduced by prophylactic insulin therapy. *Diabetes* 39:933–937, 1990
- Muir A, Peck A, Clare-Salzler M, Song YH, Cornelius J, Luchetta R, Krischer J, Maclaren N: Insulin immunization of nonobese diabetic mice induces a protective insulinitis characterized by diminished intraislet interferon-gamma transcription. *J Clin Invest* 95:628–634, 1995
- Daniel D, Wegmann DR: Protection of nonobese diabetic mice from diabetes by intranasal or subcutaneous administration of insulin peptide B-(9–23). *Proc Natl Acad Sci U S A* 93:956–960, 1996
- Karounos DG, Bryson JS, Cohen DA: Metabolically inactive insulin analog prevents type I diabetes in prediabetic NOD mice. *J Clin Invest* 100:1344–1348, 1997

22. Atkinson MA, Leiter EH: The NOD mouse model of type 1 diabetes: as good as it gets? *Nat Med* 5:601–604, 1999
23. Serreze DV, Prochazka M, Reifsnnyder PC, Bridgett MM, Leiter EH: Use of recombinant congenic and congenic strains of NOD mice to identify a new insulin-dependent diabetes resistance gene. *J Exp Med* 180:1553–1558, 1994
24. Serreze DV, Bridgett M, Chapman HD, Chen E, Richard SD, Leiter EH: Subcongenic analysis of the Idd13 locus in NOD/Lt mice: evidence for several susceptibility genes including a possible diabetogenic role for beta 2-microglobulin. *J Immunol* 160:1472–1478, 1998
25. Ikegami H, Makino S, Yamato E, Kawaguchi Y, Ueda H, Sakamoto T, Takekawa K, Ogihara T: Identification of a new susceptibility locus for insulin-dependent diabetes mellitus by ancestral haplotype congenic mapping. *J Clin Invest* 96:1936–1942, 1995
26. Ikegami H, Eisenbarth GS, Hattori M: Major histocompatibility complex-linked diabetogenic gene of the nonobese diabetic mouse: analysis of genomic DNA amplified by the polymerase chain reaction. *J Clin Invest* 85:18–24, 1990
27. Qian YW, Wang YC, Hollingsworth RE Jr, Jones D, Ling N, Lee EY: A retinoblastoma-binding protein related to a negative regulator of Ras in yeast. *Nature* 364:648–652, 1993
28. Lagaudriere-Gesbert C, Newmyer SL, Gregers TF, Bakke O, Ploegh HL: Uncoating ATPase Hsc70 is recruited by invariant chain and controls the size of endocytic compartments. *Proc Natl Acad Sci U S A* 99:1515–1520, 2002
29. Boddy MN, Howe K, Etkin LD, Solomon E, Freemont PS: PIC 1, a novel ubiquitin-like protein which interacts with the PML component of a multiprotein complex that is disrupted in acute promyelocytic leukaemia. *Oncogene* 13:971–982, 1996
30. Mannen H, Tseng HM, Cho CL, Li SS: Cloning and expression of human homolog HSMT3 to yeast SMT3 suppressor of MIF2 mutations in a centromere protein gene. *Biochem Biophys Res Commun* 222:178–180, 1996
31. Okura T, Gong L, Kamitani T, Wada T, Okura I, Wei CF, Chang HM, Yeh ET: Protection against Fas/APO-1- and tumor necrosis factor-mediated cell death by a novel protein, sentrin. *J Immunol* 157:4277–4281, 1996
32. Shen Z, Pardington-Purtymun PE, Comeaux JC, Moyzis RK, Chen DJ: UBL1, a human ubiquitin-like protein associating with human RAD51/RAD52 proteins. *Genomics* 36:271–279, 1996
33. Matunis MJ, Coutavas E, Blobel G: A novel ubiquitin-like modification modulates the partitioning of the Ran-GTPase-activating protein RanGAP1 between the cytosol and the nuclear pore complex. *J Cell Biol* 135:1457–1470, 1996
34. Yeh ET, Gong L, Kamitani T: Ubiquitin-like proteins: new wines in new bottles. *Gene* 248:1–14, 2000
35. Desterro JM, Rodriguez MS, Hay RT: SUMO-1 modification of IkappaBalpha inhibits NF-kappaB activation. *Mol Cell* 2:233–239, 1998
36. Mittrucker HW, Matsuyama T, Grossman A, Kundig TM, Potter J, Shahinian A, Wakeham A, Patterson B, Ohashi PS, Mak TW: Requirement for the transcription factor LSIRF/IRF4 for mature B and T lymphocyte function. *Science* 275:540–543, 1997
37. Rengarajan J, Mowen KA, McBride KD, Smith ED, Singh H, Glimcher LH: Interferon regulatory factor 4 (IRF4) interacts with NFATc2 to modulate interleukin 4 gene expression. *J Exp Med* 195:1003–1012, 2002